Can. J. Remote Sensing, Vol. 39, No. S1, pp. S1–S13, 2013

Predicting live and dead tree basal area of bark beetle affected forests from discrete-return lidar

Benjamin C. Bright, Andrew T. Hudak, Robert McGaughey, Hans-Erik Andersen, and José Negrón

Abstract. Bark beetle outbreaks have killed large numbers of trees across North America in recent years. Lidar remote sensing can be used to effectively estimate forest biomass, but prediction of both live and dead standing biomass in beetle-affected forests using lidar alone has not been demonstrated. We developed Random Forest (RF) models predicting total, live, dead, and percent dead basal area (BA) from lidar metrics in five different beetle-affected coniferous forests across western North America. Study areas included the Kenai Peninsula of Alaska, southeastern Arizona, north-central Colorado, central Idaho, and central Oregon, U.S.A. We created RF models with and without intensity metrics as predictor variables and investigated how intensity normalization affected RF models in Idaho. RF models predicting total BA explained the most variation, whereas RF models predicting dead BA explained the least variation, with live and percent dead BA models explaining intermediate levels of variation. Important metrics varied between models depending on the type of BA being predicted. Generally, height and density metrics were important in predicting total BA, intensity and density metrics were important in predicting live BA, and intensity metrics were important in predicting dead and percent dead BA. Several lidar metrics were important across all study areas. Whether needles were on or off beetle-killed trees at the time of lidar acquisition could not be ascertained. Future work, where needle conditions at the time of lidar acquisition are known, could improve upon our analysis and results. Although RF models predicting live, dead, and percent dead BA did not perform as well as models predicting total BA, we concluded that discrete-return lidar can be used to provide reasonable estimations of live and dead BA. Our results also showed which lidar metrics have general utility across different coniferous forest types.

Résumé. Au cours de ces dernières années, l'infestation de scolytes ont tué un grand nombre d'arbres à travers l'Amérique du Nord. La télédétection par lidar (laser) peut être utilisée pour estimer efficacement la biomasse forestière, mais la prévision de la biomasse des pieds vivants et morts dans les forêts infestées en utilisant le lidar seul reste à démontrée. Nous avons développé des Modèles de forêts aléatoires (RF) pour prédire la surface terrière (BA) totale, vivante, et le pourcentage de la surface terrière morte à partir de mesures lidar dans cinq différentes forêts de conifères touchées par les scolytes à travers l'ouest de l'Amérique du Nord. Les zones d'étude comprenaient la péninsule de Kenai en Alaska, l'Arizona du sud, le centre-nord du Colorado, le centre de l'Idaho, et le centre de l'Oregon aux Etats-Unis d'Amérique. Nous avons créé des modèles RF avec et sans mesures d'intensité comme variables prédictives et étudié les effets de la normalisation de l'intensité sur les modèles RF en Idaho. Les modèles RF prédictifs de la BA totale ont expliqué la plupart des variations tandis que les modèles RF prédictifs de la BA morte ont expliqué la moindre variation, et enfin des modèles de la BA vivante et le pourcentage de la surface terrière morte ont expliqué des niveaux intermédiaires de la variation. Des mesures importantes ont varié entre les modèles selon le type de la surface terrière en prédiction. Généralement, les mesures de la hauteur et la densité étaient importantes dans la prédiction de la BA totale, les mesures d'intensité et de densité étaient importantes dans la prédiction de la BA vivante, et enfin les mesures d'intensité étaient importantes dans la prédiction de la BA morte et son pourcentage. Plusieurs mesures du lidar ont été importantes dans toutes les zones d'étude. Que des aiguilles fussent présentes ou non-présente sur des arbres tués par les scolytes au moment de l'acquisition du lidar ne pouvait pas être établie. Les travaux à venir, où les conditions d'aiguilles au moment de l'acquisition du lidar sont connues, pourraient améliorer notre analyse et les résultats. Bien que les modèles de prédiction de la BA vivante, morte, et le pourcentage de la BA morte ne réussissent pas aussi bien que les modèles prédisant la BA totale, nous concluons que le discrete-return lidar peut être utilisé pour fournir des estimations raisonnables de BA vivante et morte. Nos résultats indiquent également que les mesures lidar ont une utilité générale dans différents types de forêts de conifères.

Received 29 December 2012. Accepted 26 June 2013. Published on the Web at http://pubs.casi.ca/journal/cjrs on 26 September 2013.

Benjamin C. Bright.[1] University of Idaho, Department of Geography, 875 Perimeter Drive MS 3021, Moscow, ID, 83844-3021, USA.

Andrew T. Hudak. USDA Forest Service, Rocky Mountain Research Station, 1221 South Main Street, Moscow, ID, 83843, USA.

Robert McGaughey, and Hans-Erik Andersen. USDA Forest Service, Pacific Northwest Research Station, University of Washington, PO Box 352100, Seattle, WA 98195-2100, USA.

José Negrón. USDA Forest Service, Rocky Mountain Research Station, 240 West Prospect, Fort Collins, CO, 80526, USA.

[1]Corresponding author (e-mail: benjamincbright@fs.fed.us).

Vol. 39, No. S1, Suppl. 1 2013

Introduction

Recent bark beetle outbreaks have killed large numbers of trees throughout western North America. Outbreaks affect ecosystem services such as carbon sequestration (Kurz et al., 2008; Hicke et al., 2012), climate regulation (Adams et al., 2010; O'Halloran et al., 2012), watershed regulation (Bethlahmy, 1974; Boon, 2009), and wildlife habitat (Chan-McLeod, 2006; Klenner and Arsenault, 2009) that forests provide. Forest managers need accurate data on beetle-induced tree mortality, preferably in the form of maps, to make better decisions on how best to remediate beetle-affected forests and restore healthy ecosystem services (Negrón et al., 2008).

Bark beetle killed trees progress through attack stages that are characterized by foliage conditions (Schmid, 1976; Wulder et al., 2006). Initially after death, trees retain green needles. Over the course of the next year or two, needles fade from green to red (in the case of mountain pine beetle caused mortality) or yellow (in the case of spruce beetle caused mortality). Eventually red or yellow needles fall and trees enter the grey stage, where most needles have fallen. Mountain pine beetles (the most widespread bark beetle currently) and spruce beetles preferentially attack larger trees (Hopping and Beall, 1948; Schmid and Frye, 1976).

Light detection and ranging (lidar), which measures forest height and density, has been successfully applied to estimate biomass and carbon stocks in healthy forests (e.g., Hudak et al., 2012) and beetle-affected forests (Bater et al., 2010; Bright et al., 2012a). In addition to height and density data, discrete-return lidar also includes intensity information, which provides some indication of the condition of the photosynthetic and nonphotosynthetic canopy elements (foliage and branches) and can be used to estimate live and dead biomass components (Kim et al., 2009; García et al., 2010). The preferential attack of large trees by bark beetles imparts a canopy structural signature that may be exploited as well (Coops et al., 2009).

Random Forest (RF), an algorithm which creates ensembles of classification trees that can be used for regression analysis of continuous variables (Breiman, 2001), has been demonstrated to be an effective modeling tool for relating forest biomass to lidar metrics (Hudak et al., 2008; Hudak et al., 2012). In addition to response variable prediction, RF provides importance measurements of explanatory variables, a feature made possible by random withholding of one-third of the data as an out-of-bag sample at every bootstrap iteration. This mitigates the need to partition data into model and validation datasets.

These features of RF are advantageous for our goal, which was to assess the sensitivity of lidar to the canopy effects of bark beetle induced tree mortality across a range of coniferous forest types. Specific objectives were (*i*) to create, evaluate, and compare RF models predicting live, dead, total, and percentage of dead basal area (BA) from lidar metrics for several areas across western North America affected by bark beetle outbreaks and (*ii*) to compare RF models between study areas to evaluate whether generalities in important explanatory variables existed. We hypothesized that density and intensity metrics would be important predictors of dead BA due to canopy changes caused by bark beetle mortality. We also hypothesized that some metrics would be consistently flagged as important in RF models across study areas. Predicting both live and dead BA in bark beetle affected forest, where live and dead trees are typically thoroughly mixed, has not been attempted before and should provide insight into the sensitivity of lidar to bark beetle effects on coniferous forest canopies.

Methods

Study areas

Study areas of bark beetle infested coniferous forest were located throughout western North America in (*i*) the Kenai Peninsula in Alaska (AK; center coordinates: 60.312°N, 150.369°W), (*ii*) the Pinaleño Mountains of southeastern Arizona (AZ; center coordinates: 32.694°N, 109.905°W), (*iii*) north-central Colorado (CO; center coordinates: 40.102°N, 105.867°W), (*iv*) central Idaho (ID; center coordinates: 44.307°N, 115.099°W), and (*v*) central Oregon (OR; center coordinates: 43.898°N, 121.332°W) (**Figure 1**). In AK and AZ, the primary mortality agents were spruce beetles, whereas in CO, ID, and OR, mountain pine beetles were responsible for tree mortality. Leading tree species varied between study areas (**Table 1**). In all study areas except AK, bark beetle infestation began roughly around 2000 and seemed to be ongoing as of 2010 according to aerial detection surveys (USDA Forest Service, 2010). Lidar data and coincident field observations acquired during or shortly after bark beetle infestation were available for each study area.

Field observations

Field observations consisted of diameter at breast height (DBH) measurements of individual trees within circular, fixed-radius plots. Field plot characteristics varied between study areas (**Table 1**). Cause of tree mortality was not always identified. Plots in AK consisted of United States Forest Service (USFS) Forest Inventory and Analysis (FIA) subplots of 7.3 m radius, whereas plots in OR consisted of both FIA and USFS Region 6 (R6) Continuous Vegetation Survey (CVS) subplots of 15.5 m radius. The subplot level data in AK and OR were combined and summarized at the plot level to preclude any issues of spatial autocorrelation, pseudo-replication, or inflated plot numbers. Individual tree DBH measurements and tree condition calls (live or dead) were summarized using the Forest Vegetation Simulator (FVS) into Live, Dead, and Total BA at the plot level, thus taking into account the different plot areas. Measurements

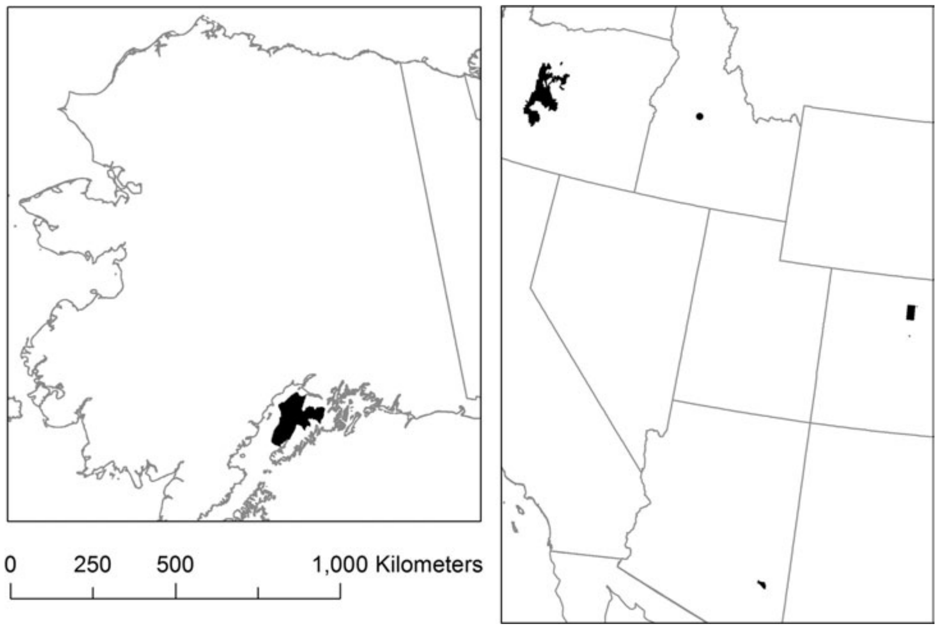

Figure 1. Location and extent of lidar acquisition areas (black polygons) in the Kenai Peninsula in Alaska, southeastern Arizona, north-central Colorado, central Idaho, and central Oregon, USA. The location of the central Idaho lidar acquisition, which was smaller in area than the other acquisitions, is marked by a black dot.

of BA were then converted from imperial units of ft^2/ac to metric units of m^2/ha. The percentage of Dead BA (%Dead BA) was derived from FVS outputs by dividing Dead BA by Total BA and multiplying by 100.

Lidar

Lidar data were acquired over the five study areas from 2008 to 2010. Lidar acquisition parameters varied between study areas (**Table 2**). For all study areas, discrete-return lidar data were delivered by vendors as LAS files, returns were classified as ground or nonground (vegetation), a bare-earth digital terrain model (DTM) was generated by interpolating ground returns, and the height above ground of vegetation returns was calculated by subtracting the bare-earth DTM height from vegetation return heights. Lidar returns within plot extents were extracted; plot extents extracted from lidar point clouds corresponded to

Table 1. Forest conditions and field characteristics of each study area.

Study area	Primary mortality agent	Leading tree species*	Infestation timespan†	Number of plots	Collection dates	Plot size (ha)	Sampling scheme
Alaska	SB	PIMA, PIGL, BENE, POTR, POTR2	1987–2000	194	2004–2009	0.07‡	Systematic
Arizona	SB	PIEN, ABLA, PSME, PIST, ABCO	2000–2010	101	2009–2010	0.05	Systematic
Colorado	MPB	PICO, ABLA, PIEN, POTR	1999–2010	113	June–August 2010	0.02	Stratified random
Idaho	MPB	PICO, ABLA, PSME, PIEN	2002–2010	27	August 2010	0.025	Stratified random
Oregon	MPB	PICO, PIPO, TSME, ABGRC, PIEN, PSME	1997–2010	158	2004–2009	0.07‡ 0.38§	Systematic

*Listed in order of abundance as measured in plots for each study area.
†Aerial detection surveys for these years indicated substantial bark beetle-caused tree mortality within the study area extent (USDA Forest Service, 2010).
‡Forest Inventory and Analysis plots consisted of four subplots with radii of 7.3 m.
§USFS Region 6 (R6) Continuous Vegetation Survey (CVS) plots consisted of five subplots with radii of 15.5 m.
Note: SB, Spruce beetle (*Dendroctonus rufipennis*); PIMA, Black spruce (*Picea mariana*); PIGL, White spruce (*Picea glauca*); BENE, Alaska paper birch (*Betula neolaskana*); POTR, Quaking aspen (*Populus tremuloides*); POTR2, Black cottonwood (*Populus trichocarpa*); PIEN, Engelmann spruce (*Picea engelmannii*); ABLA, Subalpine fir (*Abies lasiocarpa*); PSME, Douglas-fir (*Pseudotsuga menziesii*); PIST, Southwestern white pine (*Pinus strobiformis*); ABCO, White fir (*Abies concolor*); MPB, Mountain pine beetle (*Dendroctonus ponderosae*); PICO, Lodgepole pine (*Pinus contorta*); PIPO, Ponderosa pine (*Pinus ponderosa*); TSME, Mountain hemlock (*Tsuga mertensiana*); ABGRC, Grand or white fir (*Abies grandis/concolor*);

Vol. 39, No. S1, Suppl. 1 2013

Table 2. Parameters of lidar surveys for each study area.

Survey area	Vendor	Sensor	Acquisition date	Flying height above ground (m)	Sidelap (%)	Maximum scan angle (degrees)	Average pulse density (pulses/m^2)	Area (ha)
Alaska	Aerometric	Optech ALTM Gemini	May–September 2008	1800	>30	± 16	0.5 (west) and 0.11 (east)	1 223 967
Arizona	Watershed Sciences	Leica ALS50 Phase II	22–27 September 2008	1200	≥50	± 15	7.4	34 607
Colorado (nominal pulse spacing 0.7 m)	Aerometric	Optech 3100 AE	1–27 August 2010	1250	50	± 18	2	113 441
Idaho	Watershed Sciences	Leica ALS50 Phase II	4–5 August 2010	900	≥50	± 13	8.7	5 054
Oregon	Watershed Sciences	Leica ALS50 Phase II	October 2009 – September 2010	900 and 1300	50	± 14	8.6	764 111

field-measured plot extents, and thus differed in size in each study area (**Table 1**). Lidar metrics of returns within each plot were created using the Cloudmetrics tool of the FUSION software package (McGaughey, 2012). In AK and OR, the lidar points within the individual subplots were extracted and concatenated into a single file prior to calculating plot-level metrics. A total of 34 lidar metrics that included height, intensity, and density metrics were considered as candidate predictor variables (**Table 3**). Eight topographic metric grids based on bare-earth DTMs were also created using an Imagine add-on tool developed at the USFS Remote Sensing Applications Center (Ruefenacht, unpublished; http://www.fs.fed.us/eng/rsac/) (**Table 3**). Topographic metric values located at the center of each plot (or subplot in AK and OR) were extracted from 30 m resolution topographic metric grids to be used as additional predictor variables. In AK and OR, subplot values of topographic variables were averaged for each plot. Topographic metrics were included as predictor variables because we anticipated that topographic differences, such as north versus south aspects, might influence Total, Live, and Dead BA.

Intensity values varied markedly between study areas (**Figure 2**). Intensity normalization procedures as demonstrated by Korpela et al. (2010a) or Vain et al. (2010) have the potential to make intensity metrics comparable between different forest types. In our case, it was only possible to apply normalization procedures in AZ and ID. Following Korpela et al. (2010a), we used smoothed best estimated trajectory (SBET) and automatic gain control (AGC) information to normalize AZ and ID intensity values using the Boise Center Aerospace Laboratory (BCAL) LiDAR Tools software package developed at the BCAL (http://bcal.geology.isu.edu/envitools.shtml).

Random Forest modeling

We used the randomForest package in R (Breiman, 2001; Liaw and Wiener, 2002) to create RF models predicting BA. Lidar canopy and topographic metrics (**Table 3**) were considered as explanatory variables in RF models. Response variables of RF models included Total BA, Live BA, Dead BA, and %Dead BA. We created models predicting each response variable for each of the five study areas. Models excluding intensity metrics as candidate variables were also created because intensity values could not be consistently normalized in all study areas. In AZ and ID, where we were able to normalize intensity values, we created RF models that used intensity-normalized metrics for comparison with RF models that used nonintensity-normalized metrics.

In addition to creating RF models for individual study areas, we investigated the creation of generalized models that combined records from all study areas. However, significant differences (as determined by analysis of variance tests) in canopy height, canopy density, lidar intensity, and topography (**Figure 2**) that were unrelated to bark beetle effects artificially inflated variation explained by RF models generalized across the five study areas, thereby rendering them invalid. Differences in lidar survey parameters, topographic influences by study area, and infestation timing, type, and severity also made the formulation of generalized models problematic.

We identified the most important metrics based on the Model Improvement Ratio (MIR), a standardized measure of variable importance (Evans and Cushman, 2009; Evans et al., 2010). MIR scores are derived by dividing raw variable important scores (output from RF) by the maximum variable importance score, so that MIR values range from 0 to 1. MIR scores allow for variable importance comparisons among different RF models. For each of the 40 models, we ran 1000 iterations of RF that included all metrics to create distributions of MIR for each metric. Running 1000 iterations of RF produced consistent MIR distributions and avoided unnecessary processing time. To create parsimonious models, we reserved metrics for final RF models that exhibited the highest mean MIR values. Although RF randomly selects variable subsets through a bootstrapping procedure that makes it robust to highly correlated data and resistant to over-fitting (Breiman, 2001), we also eliminated one metric from highly correlated metric pairs in each model, so that final RF models did not include

Table 3. Names and descriptions of lidar and topographic metrics used as candidate variables in Random Forest models.

Metric name	Description
HMIN	Minimum canopy height
HMAX	Maximum canopy height
HMEAN	Mean canopy height
HMODE	Mode canopy height
HSD	Standard deviation of canopy height
HCV	Coefficient of variation of canopy height
HIQD	Interquartile distance of canopy height
HSKEW	Skewness of canopy height
HKURT	Kurtosis of canopy height
HP5	5th percentile of canopy height
HP10	10th percentile of canopy height
HP25	25th percentile of canopy height
HP50	50th percentile of canopy height
HP75	75th percentile of canopy height
HP90	90th percentile of canopy height
HP95	95th percentile of canopy height
CRR	Canopy relief ratio
IMIN	Minimum canopy intensity
IMAX	Maximum canopy intensity
IMEAN	Mean canopy intensity
IMODE	Mode canopy intensity
ISD	Standard deviation of canopy intensity
ICV	Coefficient of variation of canopy intensity
IIQD	Interquartile distance of canopy intensity
ISKEW	Skewness of canopy intensity
IKURT	Kurtosis of canopy intensity
DENSITY	Percentage of all returns >1.37 m in height
STRAT0	Proportion of all returns <0.15 m in height
STRAT1	Proportion of all returns ≥0.15 m and <1.37 m in height
STRAT2	Proportion of all returns ≥1.37 m and <5 m in height
STRAT3	Proportion of all returns ≥5 m and <10 m in height
STRAT4	Proportion of all returns ≥10 m and <20 m in height
STRAT5	Proportion of all returns ≥20 m and <30 m in height
STRAT6	Proportion of all returns ≥30 m in height
ELEV	Elevation
CURVPLAN	Planform curvature
CURVPROF	Profile curvature
HEAT	Heat load
SLOPE	Slope in degrees
SLPCOSA	Slope-aspect cosine transformation
SLPSINA	Slope-aspect sine transformation
TRASP	Topographic solar-radiation index

Note: Height and intensity metrics were calculated using only returns >1.37 m in height. Density and vertical strata metrics were calculated using all returns.

metrics with Pearson correlations >0.9. Final RF models that included only selected metrics were run 1000 times. We created distributions of the percent variance explained, the coefficient of determination (R^2), the root mean square error (RMSE), and the mean bias error (MBE) for each final RF model.

Results

Dead trees were least abundant in AK and OR field plots, and moderately abundant in AZ field plots. Dead trees were most abundant in CO and ID, where dead trees comprised more than half of plot-level BA (**Table 4**). Total BA of field plots averaged 16.5, 52.4, 78, 33.9, and 23.2 m^2/ha in AK, AZ, CO, ID, and OR, respectively.

RF models predicting total BA explained 36.9%–73.2% of variation in total BA (**Figure 3a**). Generally, models predicting total BA explained more variation than models predicting Live, Dead, and %Dead BA, except AZ models, where the Total BA model explained less variation than other models. Height and density metrics were important predictors of Total BA (**Tables 5** and **6**). Metrics that exhibited high MIR values in Total BA models across most study areas included: maximum canopy height, mean canopy height, a lower height percentile, the percentage of all returns >1.37 m in height, the proportion of all returns <0.15 m in height, and the proportion of all returns ≥10 m and <20 m in height. Intensity metrics were not important predictors of Total BA.

RF models predicting Live BA that included intensity metrics explained 40.2%–73.3% of variation in Live BA (**Figure 3b**). Generally, Live BA models explained less variation than Total BA models, but more variation than Dead BA models, except in AZ. In AK, ID, and OR, Live BA models explained more variation than %Dead BA models. Although still important, height metrics were not as important in predicting Live BA as in predicting Total BA (**Tables 5** and **6**). However, density metrics, namely the percentage of all returns >1.37 m in height, the proportion of all returns <0.15 m in height, and the proportion of all returns ≥10 m and <20 m in height, were important predictors of Live BA in all study areas. In areas with a higher proportion of dead BA (AZ, CO, ID; **Table 4**), intensity metrics were important predictors of Live BA (**Table 5**). When intensity metrics were removed, the percent variance explained in CO and ID Live BA models decreased from 40.2% to 16.3% and from 56.6% to 34.1%, respectively (**Figure 3a**). In AZ, where the proportion of Dead BA was more moderate, intensity metrics exhibited high MIR values, but the removal of intensity metrics only slightly decreased percent variance explained.

RF models predicting Dead BA that included intensity metrics explained 24.9%–43.8% of variation in Dead BA and generally explained less variation than models predicting Total, Live, and %Dead BA (**Figure 3c**). Intensity metrics consistently exhibited high MIR values in all areas (**Table 5**). Mean intensity, the coefficient of variation of intensity, and kurtosis of intensity metrics were important predictors of Dead BA in nearly every study area. Density metrics were also important, although density metrics with the highest MIR values varied by study area. Removing intensity metrics as candidate variables decreased percent variance explained in every study area (**Figure 3c**). As with

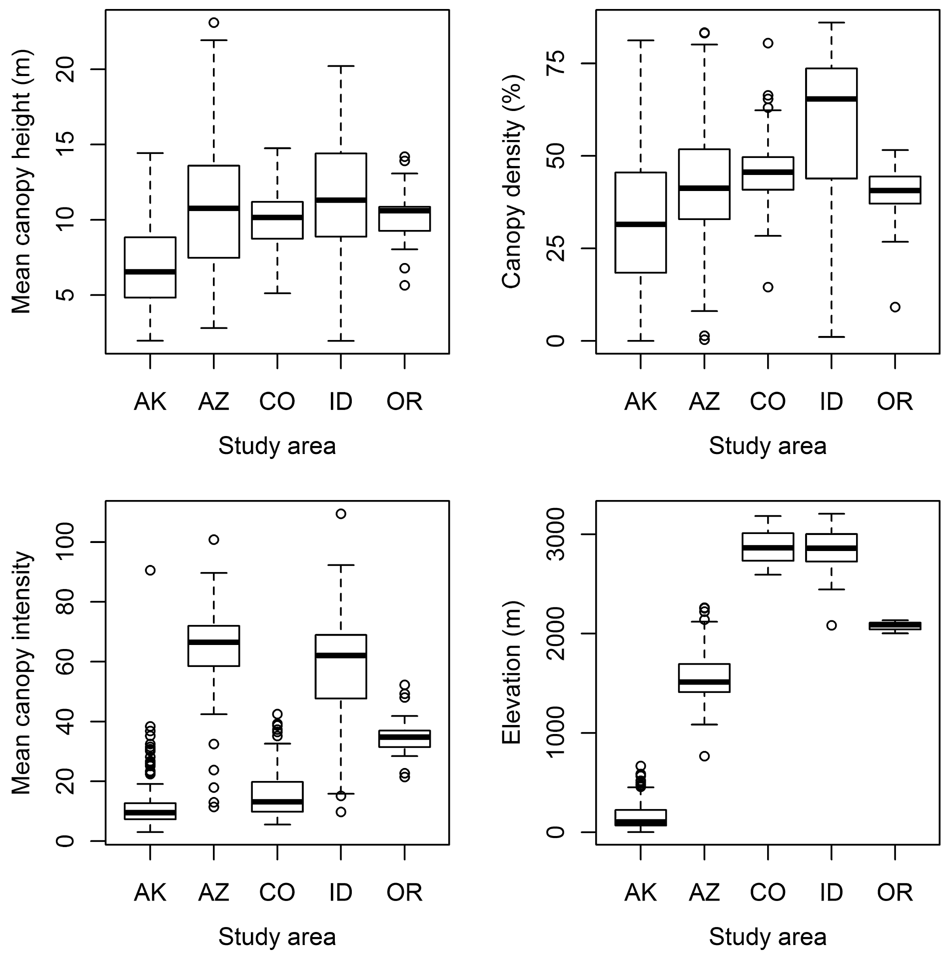

Figure 2. Study area differences in plot-level mean canopy height, canopy density, mean canopy intensity, and elevation values. Study areas include Alaska (AK), Arizona (AZ), Colorado (CO), Idaho (ID), and Oregon (OR), USA.

Table 4. Summary statistics of plot-level live and dead basal area (m^2/ha) for each study area.

Study area	Response	Minimum	1st Quartile	Median	Mean	3rd Quartile	Maximum
Alaska	Live BA	0.0	4.1	8.6	12.6	18.7	62.3
	Dead BA	0.0	0.0	1.5	3.9	5.7	24.5
Arizona	Live BA	0.0	9.3	32.8	35.5	57.0	126.3
	Dead BA	0.0	4.9	10.0	16.9	23.3	103.8
Colorado	Live BA	0.0	9.7	17.2	23.1	30.7	110.6
	Dead BA	0.0	36.8	50.8	54.9	70.6	126.7
Idaho	Live BA	5.0	8.7	14.3	15.3	21.2	29.5
	Dead BA	3.0	11.6	17.6	18.6	23.6	43.7
Oregon	Live BA	0.0	10.1	17.9	20.0	28.6	73.8
	Dead BA	0.0	0.0	1.4	3.2	4.0	29.7

Live BA models, removing intensity metrics from consideration considerably decreased the percent variance explained by Dead BA models in areas with a higher proportion of dead BA (AZ, CO, ID; **Table 4**). When intensity metrics were not included, lower height percentile metrics and height distribution dispersion and shape metrics were important in most study areas (**Table 6**).

RF models predicting %Dead BA that included intensity metrics explained 25.7%–77.5% of variation in %Dead BA (**Figure 3d**). Models predicting %Dead BA explained more variation than Dead BA models, but less variation than Total BA models. In AZ and CO, %Dead BA models explained more variation than Live BA models. As with models predicting Dead BA, mean intensity, the coefficient

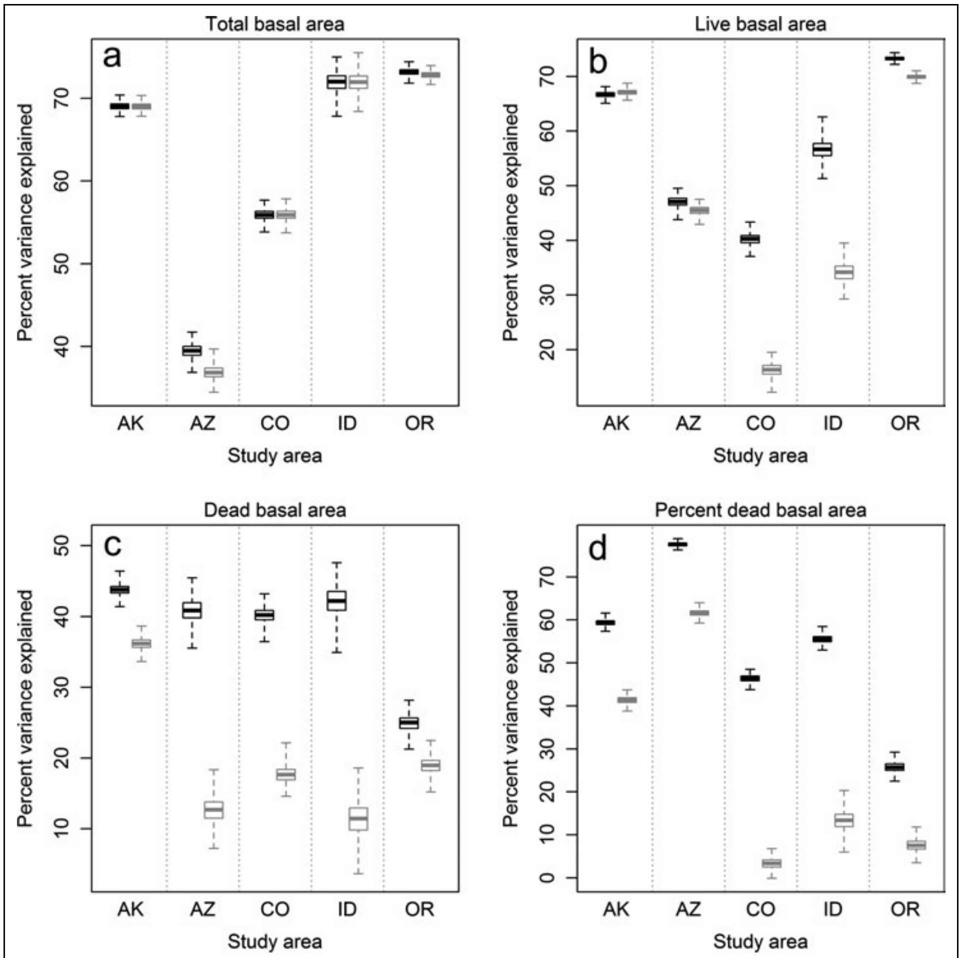

Figure 3. Distributions of percent variance explained by Random Forest (RF) models predicting Total, Live, Dead, and %Dead basal area (BA) in five study areas (Alaska, Arizona, Colorado, Idaho, and Oregon, USA). Distributions of percent variance explained come from 1000 iterations of each RF model shown in **Tables 5** and **6**. Black boxplots correspond to RF models that include intensity metrics (**Table 5**); grey boxplots correspond to RF models that do not include intensity metrics (**Table 6**).

of variation of intensity, and kurtosis of intensity metrics were important predictors of %Dead BA, and the removal of these important intensity metrics greatly decreased percent variance explained in all study areas (**Figure 3d**). Height and density metrics explained much less variation in %Dead BA than intensity metrics (**Table 6**).

Elevation was frequently an important variable in all models and all study areas (**Table 5**). Other topographic variables were not as important. When intensity metrics were removed from consideration, slope and aspect variables occasionally exhibited high MIR values (**Table 6**).

Intensity normalization in ID did not greatly affect variance explained by RF models predicting Total and Live BA (**Table 7**); however, intensity normalization increased variance explained by RF models predicting Dead and %Dead BA (**Table 7**). AZ results were equivocal, possibly due to AGC and intensity inaccuracies caused by a scanner malfunction; thus, we did not report AZ results.

Discussion

RF models explained the most variation in Total BA and the least variation in Dead BA. RF models predicting Live and %Dead BA explained intermediate levels of variation. We attribute the lower variance explained for Dead BA compared with Live and Total BA to the fact that lidar height and density metrics were primarily measuring total standing tree canopy structure, regardless of condition.

Tree condition calls (live or dead) at the time of field data collection did not coincide with the time of lidar acquisition; thus, we cannot be certain whether dying or dead trees were green, red, or yellow (needles on), or grey (needles off) when the lidar was collected. Temporal mismatches between the lidar acquisitions and field data collection limited our analysis and likely contributed to inaccuracy in RF models, especially those predicting Live, Dead, and %Dead BA. A similar analysis that controls for dead tree conditions,

Table 5. Random Forest models predicting Total, Live, Dead, and%Dead basal area for Alaska, Arizona, Colorado, Idaho, and Oregon, USA.

	Total BA					Live BA					Dead BA					%Dead BA				
	AK	AZ	CO	ID	OR	AK	AZ	CO	ID	OR	AK	AZ	CO	ID	OR	AK	AZ	CO	ID	OR
R^2	0.691	0.396	0.560	0.776	0.738	0.669	0.471	0.404	0.623	0.735	0.439	0.422	0.417	0.448	0.251	0.601	0.777	0.467	0.557	0.264
RMSE	7.0	23.7	19.5	4.9	8.2	6.8	21.0	15.5	4.8	7.0	4.1	14.6	21.0	7.5	4.4	19.4	16.2	16.2	13.4	15.7
MBE	–0.05	0.68	–0.65	–0.20	–0.05	–0.05	–0.25	–0.39	–0.32	–0.09	–0.14	0.06	–0.39	0.09	–0.08	–0.05	–0.36	–0.18	0.57	0.16
Variables (no.)	7	5	7	5	8	8	9	9	10	6	11	8	9	5	8	12	6	3	2	5
Variables																				
HMAX	0.3		0.2	0.2				0.1	0.1		0.6		0.2		0.4					
HMEAN	0.1	0.3	0.2		0.1			0.1		0.1	0.1		0.2							
HMODE		0.5																		
HSD																0.2				
HCV											0.1					0.2				
HIQD											0.1									
HSKEW														0.1						
HP10							0.2													
HP25			0.1		0.1	0.1								0.1		0.1				
HP75				0.5		0.1														
CRR											0.2					0.1				
IMAX																0.5				
IMEAN							0.5	0.2	0.2		0.2	0.9			0.6	1.0	1.0	0.1		0.4
ISD		0.2									1.0				0.9					
ICV						0.1	0.2	0.1	0.6		0.2	1.0	0.7	0.9	0.9	0.4	0.8	0.8	0.8	1.0
IIQD					0.1		0.3			0.1		0.2					0.2			0.3
ISKEW						0.1					0.1									
IKURT								1.0	0.9			0.3	0.6	0.6	0.6	0.1	0.1	0.8	0.9	0.6
DENSITY	0.9	1.0	1.0	0.3	1.0	1.0	1.0	0.6	0.7	1.0		0.2	0.6		0.7					
STRAT0	0.4	0.4	0.2	0.2	0.2	0.3	0.2	0.2	0.5	0.2			0.1							
STRAT1							0.9				0.3	0.2				0.1	0.1			
STRAT3	0.3					0.4			0.1				0.2							
STRAT4	1.0		0.4	1.0	0.6	0.8	0.2	0.3	0.2	1.0	0.1		0.4	0.1		0.1				
STRAT5					0.4			0.1	0.1	0.3		0.2			0.7					
ELEV	0.1		0.1		0.1		0.6		0.1		0.4	0.4	0.2		0.5	0.5	0.7			0.4

Note: R^2, RMSE, MBE, number of variables, selected variables, and model improvement ratio (MIR) values for selected variables are shown. R^2, RMSE, MBE, and MIR values are means of 1000 Random Forest iterations. MIR values range from 0 to 1, where 1 indicates most important. Shading indicates metrics that were chosen across at least four study areas. (BA, basal area; AK, Alaska; AZ, Arizona; CO, Colorado; ID, Idaho; OR, Oregon; R^2, coefficient of determination; RMSE, root mean square error; MBE, mean bias error (MBE). See **Table 3** for variable names and descriptions.)

Table 6. Random Forest models predicting Total, Live, Dead, and%Dead basal area for Alaska, Arizona, Colorado, Idaho, and Oregon, USA.

	Total BA					Live BA					Dead BA					%Dead BA				
	AK	AZ	CO	ID	OR	AK	AZ	CO	ID	OR	AK	AZ	CO	ID	OR	AK	AZ	CO	ID	OR
R^2	0.691	0.369	0.561	0.776	0.733	0.672	0.455	0.179	0.342	0.702	0.363	0.132	0.184	0.125	0.192	0.422	0.617	0.052	0.135	0.086
RMSE	7.0	24.2	19.5	4.9	8.2	6.8	21.3	18.4	6.0	7.5	4.4	17.7	24.6	9.3	4.5	23.3	21.2	21.7	18.7	17.5
MBE	−0.05	0.83	−0.63	−0.20	−0.08	−0.06	−0.46	−0.43	−0.15	−0.03	−0.14	−0.28	−0.32	0.51	−0.05	−0.32	−0.33	−0.11	−0.40	−0.01
Varaibles (no.)	7	5	7	5	7	7	9	9	5	5	9	9	8	5	7	12	6	5	3	5
Variables																				
HMAX	0.3		0.2	0.2				0.1			0.6		0.4		0.5	0.1				
HMEAN	0.1	0.4	0.2		0.2			0.1		0.2	0.1		0.6			0.2				
HMODE		0.5						0.1				0.3								
HSD																				0.5
HCV							0.2					0.3				0.3				
HIQD											0.1	0.4				0.1				
HSKEW											0.1		0.2	0.6				0.7		0.3
HKURT																		0.6		0.6
HP5											0.2									
HP10							0.3					0.3	0.3				0.1			
HP25			0.1		0.2	0.1	0.2													
HP75				0.5		0.1								0.7	0.9					
CRR											0.2					0.2		0.6		
DENSITY	0.9	1.0	1.0	0.3	1.0	1.0	1.0	1.0	1.0	1.0		0.5	0.6		0.5	0.2	0.1			0.7
STRAT0	0.4	0.4	0.2	0.2	0.3	0.3	0.2	0.4	0.7	0.2				0.5		0.1				
STRAT1							0.9				0.3	0.9				0.1	0.3			
STRAT2																				
STRAT3	0.3					0.4	0.2	0.1	0.3				0.5			0.1	0.1	0.8		
STRAT4	1.0	0.3	0.4	1.0	0.7	0.8	0.2	0.4	0.3	0.9	0.2		1.0	0.8	0.3	0.1	0.1			
STRAT5					0.5			0.1		0.4		0.5			1.0					
STRAT6															0.5					
ELEV	0.1		0.1		0.2	0.1	0.7		0.5		1.0	0.9	0.5		0.4	1.0	1.0		1.0	1.0
CURVPLAN														0.6						
SLOPE								0.1								0.1		0.9		
SLPCOSA												0.4								
TRASP																			0.2	

Note: Intensity metrics were not included as candidate variables. R^2, RMSE, MBE, number of variables, selected variables, and model improvement ratio (MIR) values for selected variables are shown. R^2, RMSE, MBE, and MIR values are means of 1000 RF iterations. MIR values range from 0 to 1, where 1 indicates most important. Shading indicates metrics that were chosen across at least four study areas. (BA, basal area; AK, Alaska; AZ, Arizona; CO, Colorado; ID, Idaho; OR, Oregon;R^2, coefficient of determination; RMSE, root mean square error; MBE, mean bias error (MBE). See **Table 3** for variable names and descriptions.)

Table 7. Average percent variance explained by Random Forest models predicting basal area in Idaho using original versus intensity values normalized by range and automatic gain control.

Response	Total BA		Live BA		Dead BA		%Dead BA	
Intensity metrics	Original	Normalized	Original	Normalized	Original	Normalized	Original	Normalized
Percent variance explained	72.0	72.3	56.6	55.9	42.2	48.0	55.5	67.8

Note: Percent variance explained values shown are averages from 1000 RF models. (BA, basal area.)

especially the amount of needles on dead trees, at the time of lidar acquisition would provide more information on the capability of lidar to predict live and dead basal area in beetle-affected forests. Discrepancies between field and lidar data collections were greater in AK and OR because only a nominal 10%–20% of FIA or CVS plots are characterized in a given year (O'Connell et al., 2012). We eliminated from consideration any field plots that were visited more than five years prior to the lidar collection, which resulted in the elimination of 32 plots in OR. This decision was based on the findings of Mitchell and Preisler (1998) that tree fall rates increase substantially five years after bark beetle induced mortality.

Metrics of all types (height, intensity, density, and topographic) helped to explain variation in BA. Many metrics were important across the study areas (**Tables 5** and **6**). In general, height and density metrics were most important in predicting Total BA, intensity and density metrics were most important in predicting Live BA, and intensity metrics were most important in predicting Dead and %Dead BA. The relative importance of metrics used to predict Live, Dead, and %Dead BA likely differed depending on whether beetle-killed trees were red or yellow (needles on) or grey (needles off); however; temporal mismatches between lidar acquisitions and field data collection did not allow us to investigate how tree attack stage affected BA prediction. Lidar pulses should penetrate further into grey forest canopies than red or yellow forest canopies; therefore, height and density metrics should be different and vary in importance depending on the amount of needles remaining on beetle-killed trees. Lidar intensity is likely influenced by tree attack stage as well. The percentage of all returns >1.37 m in height (DENSITY) and the proportion of all returns <0.15 m in height (STRAT0) were important predictors of Total and Live BA because these metrics are good indicators of canopy cover; STRAT0 is an indicator of canopy gap fraction and is strongly, negatively correlated to DENSITY. Elevation was often an important predictor of BA and likely acted as a proxy for forest composition. In ID, Dead BA tended to decrease with elevation increase because forest composition at higher elevations included more nonhost species that were not killed by bark beetles (Bright et al., 2012b). In all other study areas, the relationship between elevation and Dead BA was opposite to that of ID; Dead BA tended to increase with elevation increase and often an increased prevalence of host tree species, such as in AZ where susceptible spruce trees occur at the higher elevations.

Lidar intensity measures the magnitude of energy reflected back to the lidar sensor. Canopy conditions such as foliage reflectance and density influence lidar intensity (Korpela et al., 2010a). However, intensity values are also dependent on instrument, view angle, flying height, and study area (**Figure 2**); these limitations should be considered when interpreting lidar intensity values. We found that the importance of intensity metrics depended on the proportion of Dead BA in each study area; in areas of greater tree mortality, intensity metrics tended to be more important in predicting Live, Dead, and %Dead BA. Spruce beetle mortality in AK and AZ was less severe than mountain pine beetle mortality in CO and ID; hence, intensity metrics were more important predictors of mountain pine beetle caused tree mortality. Lidar intensity values tended to decrease as dead BA proportion increased within a given study area, likely because of decreasing foliage and increasing woody material content (Kim et al., 2009); as such, lidar intensity might be a more important predictor of grey BA than yellow or red BA.

Discrete-return lidar systems often record multiple returns from a given pulse; intensity is dependent on return number. The first target object struck by the laser pulse has 100% of the energy available for reflection and detection by the receiver. The amount of energy available as subsequent target objects are struck by the same pulse depends on the amount reflected by the first target. We used intensity values from all returns to compute intensity metrics. However, model performance might be improved if we used only first returns to compute intensity metrics, thereby eliminating the confounding effect of return number. Others have reported that using only intensity values from first returns improves biomass prediction (Kim et al., 2009) and tree species classification (Ørka et al., 2009; Korpela et al., 2010b). Kim et al. (2009) found that models predicting biomass that used only first returns predicted biomass more accurately in northern AZ, likely because open canopy conditions allowed laser pulses to reach the ground so that first returns sufficiently represented canopy structure. Canopies in most of our study areas were likely less open, however, so using only first returns (which might not have penetrated to the ground) for height and density metrics might not have improved model performance in our case. Intensity normalization in ID improved RF models predicting Dead and %Dead BA, demonstrating that the use of intensity for distinguishing dead versus live canopies and intensity normalization procedures need to be further researched. Intensity normalization was not possible for AK, CO, and

OR lidar surveys, possibly limiting our ability to apply RF models and map BA across these study areas. We encourage those who acquire lidar for bark beetle applications to consider a lidar system that gathers AGC information and to specify that SBET files and AGC information are included in the contract.

Differences in field observations and lidar surveys between study areas could have affected comparisons of model prediction accuracy between study areas. Co-registration error between field observations and coincident lidar point samples can affect forest BA prediction accuracy (Frazer et al., 2011). Larger plots are more resistant to co-registration error and plot edge effects (i.e., tree crowns along plot edges leaning into or out of plot extents) that decrease the accuracy of predicting basal area and related forest attributes. Our plot sizes and corresponding lidar point cloud sizes differed between study areas (**Table 1**); thus, plot size differences may have affected percent variance explained and partly confounded comparisons of prediction accuracy between study areas. Similarly, differing plot sample sizes between study areas might have also affected comparisons of prediction accuracy between study areas. Finally, point density was lower in the AK and CO lidar surveys. Lower point density of the CO lidar survey could have decreased prediction accuracy of CO models relative to models of other study areas. However, lower point density in AK did not decrease AK model performance relative to other study areas. Lower point density does not necessarily affect prediction accuracy of basal area and related forest attributes (Hudak et al., 2012).

Our results confirm the utility of lidar for the prediction of forest BA that has been demonstrated in other studies. Similar to Hudak et al. (2012) and Bright et al. (2012a), we found upper percentile height, mean canopy height, canopy cover metrics, and upper density strata metrics to be effective predictors of total forest BA. Like Kim et al. (2009), we found that lidar intensity metrics were important predictors of dead and live forest BA. Kim et al. (2009) used high and low peaks of intensity probability distributions to estimate live and dead biomass, respectively; our approach did not make use of these metrics but despite our use of different, perhaps less precise intensity metrics, we, like Kim et al. (2009), found that lower intensity values were associated with Dead BA, whereas higher intensity values were associated with Live BA. Although intensity metrics were more effective predictors of Dead and %Dead BA, we found measures of height distribution dispersion and shape to be the most important predictors of Dead and %Dead BA when intensity metrics were not included as candidate variables. Similarly, Bater et al. (2009) found the coefficient of variation of lidar height to be the most important predictor of dead standing tree proportion. Also, Martinuzzi et al. (2009) found the median absolute deviation of height to be an important predictor of the presence of snags. These results point to greater penetration of laser pulses into defoliated canopies, broadening metrics of height variability. Because greater penetration of laser pulses into the canopy is an important indicator of Dead BA, our approach might predict Dead BA more accurately in defoliated forests, rather than recently attacked forests.

Conclusion

Estimation of plot-level live and dead structural attributes in beetle-affected coniferous forest using lidar alone has not been demonstrated previously. We showed that lidar can be used to estimate both Live and Dead BA within beetle-affected forest. RF provided a useful tool for assessing the importance of lidar metrics. We created RF models predicting Total, Live, Dead, and %Dead BA in five study areas across western North America; some lidar metrics were important across coniferous forest types. Height and density metrics were important predictors of total BA, intensity and density metrics were important predictors of Live BA, and intensity metrics were important predictors of Dead and %Dead BA. Differences between lidar acquisition timing and field observation collection timing, however, limited the interpretation of our results. Further work that considers needle conditions (i.e., presence or absence of needles) of beetle-killed trees at the time of lidar acquisition would provide a more thorough analysis of the capability of lidar to predict Live and Dead basal area in bark beetle-affected forests.

Bark beetle caused tree mortality pervades western North America (Meddens et al., 2012). As such, many forest managers need information about bark beetle impacts on forests. Our study is of value to forest managers who wish to quantify bark beetle impacts on coniferous forest canopy BA wherever coincident lidar data are available.

Acknowledgements

Funding was provided by the Special Technology Development Program of the U.S. Forest Service Forest Health Protection division. Funding to the University of Idaho was provided through Joint Venture Agreement 11-JV-11221633-184. We thank Craig Wilcox, Kit O'Connor, and Dr. Ann Lynch for providing Arizona field plot data; Drs. Jenny Briggs and Todd Hawbaker for providing Colorado field plot and lidar data; and Dr. Harold Zald for cleaning the Oregon plot data. We also thank Dr. Jeff Hicke for productive discussions relating to this study, Dr. Rupesh Shrestha for help with intensity normalization methods, and Jean-Paul Ntore Nduwayo for translating the abstract into French.

References

Adams, H.D., Macalady, A.K., Breshears, D.D., Allen, C.D., Stephenson, N.L., Saleska, S.R., Huxman, T.E., and McDowell, N.G. 2010. Climate-induced tree mortality: earth system consequences. *EOS Transactions*, Vol. 91, pp. 153–154. doi: 10.1029/2010EO170003.

Bater, C.W., Coops, N.C., Gergel, S.E., LeMay, V., and Collins, D. 2009. Estimation of standing dead tree class distributions in northwest coastal forests using lidar remote sensing. *Canadian Journal of Forest Research*, Vol. 39, pp. 1080–1091. doi: 10.1139/X09-030.

Bater, C.W., Wulder, M.A., White, J.C., and Coops, N.C. 2010. Integration of LIDAR and digital aerial imagery for detailed estimates of Lodgepole Pine (*Pinus contorta*) volume killed by Mountain Pine Beetle (*Dendroctonus ponderosae*). *Journal of Forestry*, Vol. 108, pp. 111–119.

Bethlahmy, N. 1974. More streamflow after a bark beetle epidemic. *Journal of Hydrology*, Vol. 23, pp. 185–189. doi: 10.1016/0022-1694(74)90001-8.

Boon, S. 2009. Snow ablation energy balance in a dead forest stand. *Hydrological Processes*, Vol. 23, pp. 2600–2610. doi: 10.1002/hyp.7246.

Breiman, L. 2001. Random forests. *Machine Learning*, Vol. 45, pp. 5–32. doi: 10.1023/A:1010933404324.

Bright, B.C., Hicke, J.A., and Hudak, A.T. 2012a. Estimating aboveground carbon stocks of a forest affected by mountain pine beetle in Idaho using lidar and multispectral imagery. *Remote Sensing of Environment*, Vol. 124, pp. 270–281. doi: 10.1016/j.rse.2012.05.016.

Bright, B.C., Hicke, J.A., and Hudak, A.T. 2012b. Landscape-scale analysis of aboveground tree carbon stocks affected by mountain pine beetles in Idaho. *Environmental Research Letters*, Vol. 7, No. 4, 045702. doi: 10.1088/1748-9326/7/4/045702.

Chan-McLeod, A.C.A. 2006. A review and synthesis of the effects of unsalvaged mountain-pine-beetle-attacked stands on wildlife and implications for forest management. *BC Journal of Ecosystems and Management*, Vol. 7, pp. 119–132.

Coops, N.C., Varhola, A., Bater, C.W., Teti, P., Boon, S., Goodwin, N., and Weiler, M. 2009. Assessing differences in tree and stand structure following beetle infestation using lidar data. *Canadian Journal of Remote Sensing*, Vol. 35, pp. 497–508. doi: 10.5589/m10-005.

Evans, J.S., and Cushman, S.A. 2009. Gradient modeling of conifer species using Random Forests. *Landscape Ecology*, Vol. 5, pp. 673–683. doi: 10.1007/s10980-009-9341-0.

Evans, J.S., Murphy, M.A., Holden, Z.A., and Cushman, S.A. 2010. Modeling species distribution and change using Random Forests, Chapter 8. In *Predictive Modeling in Landscape Ecology.* Edited by C.A. Drew, F. Huettmann, Y. Wiersma. Springer, New York, New York, USA. pp. 139–159.

Frazer, G.W., Magnussen, S., Wulder, M.A., and Niemann, K.O. 2011. Simulated impact of sample plot size and co-registration error on the accuracy and uncertainty of LiDAR-derived estimates of forest stand biomass. *Remote Sensing of Environment*, Vol. 115, pp. 636–649. doi: 10.1016/j.rse.2010.10.008.

García, M., Riaño, D., Chuvieco, E., and Danson, F.M. 2010. Estimating biomass carbon stocks for a Mediterranean forest in central Spain using LiDAR height and intensity data. *Remote Sensing of Environment*, Vol. 114, pp. 816–830. doi: 0.1016/j.rse.2009.11.021.

Hicke, J.A., Allen, C.D., Desai, A.R., Dietze, M.C., Hall, R.J., Hogg, E.H., Kashian, D.M., Moore, D., Raffa, K.F., Sturrock, R.N., and Vogelmann, J. 2012. Effects of biotic disturbances on forest carbon cycling in the United States and Canada. *Global Change Biology*, Vol. 18, pp. 7–34. doi: 10.1111/j.1365-2486.2011.02543.x.

Hopping, G.R., and Beall, G. 1948. The relation of diameter of lodgepole pine to incidence of attack by the bark beetle *Dendroctonus monticolae* Hopkins. *Forestry Chronicle*, Vol. 24, pp. 141–145.

Hudak, A.T., Crookston, N.L., Evans, J.S., Hall, D.E., and Falkowski, M.J. 2008. Nearest neighbor imputation of species-level, plot-scale forest structure attributes from LiDAR data. *Remote Sensing of Environment*, Vol. 112, pp. 2232–2245. doi: 10.1016/j.rse.2007.10.009.

Hudak, A.T., Strand, E.K., Vierling, L.A., Byrne, J.C., Eitel, J., Martinuzzi, S., and Falkowski, M.J. 2012. Quantifying aboveground forest carbon pools and fluxes from repeat LiDAR surveys. *Remote Sensing of Environment*, Vol. 123, pp. 25–40. doi: 10.1016/j.rse.2012.02.023.

Kim, Y., Yang, Z., Cohen, W.B., Lauver, C.L., and Vankat, J.L. 2009. Distinguishing between live and dead standing tree biomass on the North Rim of Grand Canyon National Park, USA using small-footprint lidar data. *Remote Sensing of Environment*, Vol. 113, pp. 2499–2510. doi: 10.1016/j.rse.2009.07.010.

Klenner, W., and Arsenault, A. 2009. Ponderosa pine mortality during a severe bark beetle (*Coleoptera: Curculionidae, Scolytinae*) outbreak in southern British Columbia and implications for wildlife habitat management. *Forest Ecology and Management*, Vol. 258S, pp. S5–S14. doi: 10.1016/j.foreco.2009.08.035.

Korpela, I., Ørka, H.O., Hyyppä, J., Heikkinen, V., and Tokola, T. 2010a. Range and AGC normalization in airborne discrete-return LiDAR intensity data for forest canopies. *ISPRS Journal of Photogrammetry and Remote Sensing*, Vol. 65, pp. 369–379. doi:10.1016/j.isprsjprs.2010.04.003.

Korpela, I., Ørka, H.O., Maltamo, M., Tokola, T., and Hyyppä, J. 2010b. Tree species classification using airborne LiDAR – effects of stand and tree parameters, downsizing of training set, intensity normalization, and sensor type. *Silva Fennica*, Vol. 44, No. 2, pp. 319–339.

Kurz, W.A., Dymond, C.C., Stinson, G., Rampley, G.J., Neilson, E.T., Carroll, A.L., Ebata, T., and Safranyik, L. 2008. Mountain pine beetle and forest carbon feedback to climate change. *Nature*, Vol. 452, pp. 987–990. doi: 10.1038/nature06777.

Liaw, A., and Wiener, M. 2002. Classification and Regression by randomForest. *R News*, Vol. 2, No. 3, pp. 18–22.

Martinuzzi, S., Vierling, L.A., Gould, W.A., Falkowski, M.J., Evans, J.S., Hudak, A.T., and Vierling, K.T. 2009. Mapping snags and understory shrubs for a LiDAR-based assessment of wildlife habitat suitability. *Remote Sensing of Environment*, Vol. 113, pp. 2533–2546. doi: 10.1016/j.rse.2009.07.002.

McGaughey, R.J. 2012. *FUSION/LDV: Software for LIDAR Data Analysis Visualization*. USDA Forest Service, Pacific Northwest Research Station, Portland, Oregon, USA.

Meddens, A.J.H, Hicke, J.A., and Ferguson C.A. 2012. Spatial and temporal patterns of observed bark beetle-caused tree mortality in British Columbia and the western US. *Ecological Applications*, Vol. 22, pp. 1876–1891. doi: 10.1890/11-1785.1.

Mitchell, R.G., and Preisler, H.K. 1998. Fall rate of lodgepole pine killed by the mountain pine beetle in central Oregon. *Western Journal of Applied Forestry*, Vol. 13, pp. 23–26.

Negrón, J.F., Allen, K., Cook, B., and Withrow, J.R. Jr. 2008. Susceptibility of ponderosa pine, *Pinus ponderosa* (Dougl. Ex Laws.), to mountain pine beetle, *Dendroctonus ponderosae* Hopkins, attack in uneven-aged stands in the Black Hills of South Dakota and Wyoming USA. *Forest Ecology and Management*, Vol. 254, pp. 327–334. doi: 10.1016/j.foreco.2007.08.018.

O'Connell, B.M., LaPoint, E.B., Turner, J.A., Ridley, T., Boyer, D., Wilson, A.M., Waddell, K.L., Christensen, G., and Conkling, B.L. 2012.

The Forest Inventory and Analysis Database: Database Description and Users Manual Version 5.1.2 for Phase 2. USDA Forest Service. Available from http://www.fia.fs.fed.us/library/database-documentation/ [cited November 2012].

O'Halloran, T.L., Law, B.E., Goulden, M.L., Wang, Z., Barr, J.G., Schaaf, C., Brown, M., Fuentes, J.D., Göckede, M., Black, A., and Engel, V. 2012. Radiative forcing of natural forest disturbances. *Global Change Biology*, Vol. 18, pp. 555–565. doi: 10.1111/j.1365-2486.2011.02577.x.

Ørka, H.O., Næsset, E., and Bollandsås, O.M. 2009. Classifying species of individual trees by intensity and structure features derived from airborne laser scanner data. *Remote Sensing of Environment*, Vol. 113, pp. 1163–1174. doi: 10.1016/j.rse.2009.02.002.

Schmid, J.M., and Frye, R.H. 1976. *Stand ratings for spruce beetles.* USDA Forest Service Rocky Mountain Forest and Range Experiment Station, Fort Collins, Colorado, USA, Research Note RM-309.

Schmid, J.M. 1976. *Temperatures, growth, and fall of needles on Engelmann spruce infested by spruce beetles.* USDA Forest Service Rocky Mountain Forest and Range Experiment Station, Fort Collins, Colorado, USA. Research Note RM-331.

USDA Forest Service. 2010. *Major forest insect and disease conditions in the United States: 2009 update.* Forest Health Protection, Washington D.C., USA. FS–952.

Vain, A., Yu, X., Kaasalainen, S., and Hyyppä, J. 2010. Correcting Airborne Laser Scanning Intensity Data for Automatic Gain Control Effect. *IEEE Geoscience and Remote Sensing Letters*, Vol. 7, pp. 511–514. doi: 10.1109/LGRS.2010.2040578.

Wulder, M.A., Dymond, C.C., White, J.C., Leckie, D.G., and Carroll, A.L. 2006. Surveying mountain pine beetle damage of forests: A review of remote sensing opportunities. *Forest Ecology and Management*, Vol. 221, pp. 27–41. doi: 10.1016/j.foreco.2005.09.021.